Long–Chain Terminal Alcohols Through Catalytic CO Hydrogenation.

7 AUTHORS, INCLUDING:

Peter V Liddicoat
Atomnaut Inc.
11 PUBLICATIONS **316** CITATIONS

SEE PROFILE

Peter Johann Felfer
Friedrich-Alexander-University of Erlangen-Nü…
28 PUBLICATIONS **212** CITATIONS

SEE PROFILE

Simon Ringer
University of Sydney
351 PUBLICATIONS **7,868** CITATIONS

SEE PROFILE

Norbert Kruse
Washington State University
191 PUBLICATIONS **2,442** CITATIONS

SEE PROFILE

Long-Chain Terminal Alcohols through Catalytic CO Hydrogenation

Yizhi Xiang,[†] Véronique Chitry,[†] Peter Liddicoat,[‡] Peter Felfer,[‡] Julie Cairney,[‡] Simon Ringer,[‡] and Norbert Kruse*,[†]

[†]Chemical Physics of Materials (Catalysis-Tribology), Université Libre de Bruxelles, Campus Plaine, CP 243, 1050 Brussels, Belgium

[‡]Australian Centre for Microscopy & Microanalysis, and School of Aerospace, Mechanical & Mechatronic Engineering, The University of Sydney, NSW 2006, Australia

S *Supporting Information*

ABSTRACT: We show that long-chain 1-alcohols can be produced with high selectivities using heterogeneous CO hydrogenation catalysis. This breakthrough is achieved through the targeted design of "CoCuMn" nanosized core—shell particles using co-precipitation of metal salts into oxalate precursors and subsequent thermal decomposition. Using stoichiometric CO/H_2 feeds, the selectivities to 1-alcohols or combined 1-alcohols/1-alkenes are usually higher than 60% and occasionally up to 95%. The Anderson—Schulz—Flory chain-lengthening probabilities for these products are higher than 0.6, but usually below 0.9 so as to optimize the C_8—C_{14} slate as feedstock for plasticizers, lubricants, or detergents.

The production of terminal 1-alcohols is a large-scale industrial process of homogeneous catalysis. Basically two chemical transformations occur in sequence: hydroformylation of a C_n ($n \geq 3$) 1-alkene and hydrogenation of the C_{n+1} aldehyde to the respective alcohol. Alternatively, avoiding homologation, a C_n ($n \geq 2$) 1-alkene can be hydrated to a C_n terminal alcohol using acidic catalysis. A problematic issue of this latter process is the limited regioselectivity since according to the Markovnikov rule the protonation of the double bond disfavors transition states amenable to form primary alcohols. Much has been learned though, over many years of applied and fundamental research, about how to tune the regioselectivity by configuring the organometallic catalysts using specific ligands.[1]

Recent efforts have aimed at developing one-pot tandem strategies for 1-alcohol production from terminal alkenes. The group of Grubbs[2] reported a cooperative two-catalyst system by coupling a Wacker-type oxidation process to a reduction cycle and obtained good selectivities of anti-Markovnikov products. One-pot hydroformylation/hydrogenation with one-[3] and two-catalyst[4] systems was also found to produce 1-alcohols with high selectivities and yields. While fighting the Markovnikov rule in the homogeneous phase reaction is one issue of catalyst development, the noble metal recovery is another one. With this background it is worth exploring a research strategy using heterogeneous catalysis by starting from syngas and enforcing hydrocarbon chain lengthening in a Fischer—Tropsch (FT) process over base transition metals.

It is interesting to note that the first report on oxygenates ("synthol") production via heterogeneous CO hydrogenation goes back to the pioneering work of Fischer and Tropsch.[5]

Later, after Roelen had explored the prospects for recycling "gasol" (light hydrocarbons, including olefins and, in particular, ethylene, for which there was no subsequent use at that time—unlike the present-day situation) so as to increase the chain lengthening during the heterogeneous FT synthesis over Co-based catalysts, it became clear that oxygenates and, in particular, aldehydes were produced by hydroformylation.[6] Despite this major discovery, it escaped Roelen's attention that this reaction was actually a case of homogeneous rather than heterogeneous catalysis. The generation of tetracarbonylhydridocobalt, $HCo(CO)_4$, as the active catalyst in an overall homogeneous reaction was finally proven in the work of Wender et al.,[7] while the catalytic reaction mechanism was first set up by Heck and Breslow.[8]

In the present paper we report on the production of long-chain 1-alcohols according to the heterogeneous FT technology. Following on from an earlier cooperation with ExxonMobil,[9] we demonstrate that ternary "CoCuMn" metal catalysts can be tuned so as to strongly favor product slates of straight hydrocarbons with terminal functionalization over "simple" paraffins. In particular, nanosized core—shell particles with tailored shell compositions are synthesized by oxalate co-precipitation so as to maximize the yield of C_8—C_{14} terminal alcohols as feedstock for plasticizers, surfactants, detergents, and so on. One of the reasons for using the "oxalate route" of catalyst preparation is associated with the capability of the oxalate anion to coordinate with a number of transition metals so as to create polymeric structures.[10] It may then be hoped that oxalate co-precipitation of several metals at a time will lead to the formation of mixed-metal-oxalate units as building blocks of a common framework structure which decomposes into nanosized, mixed-metal particles upon mild heating.

From an experimental point of view, oxalates were co-precipitated from oxalic acid and nitrate precursors in acetone (see Supporting Information (SI)). They were subsequently transformed into catalysts by temperature-programmed decomposition in flowing hydrogen (H_2-TPDec). The spectral features thus obtained turned out to be rather different from those of the pure single-metal oxalates, allowing a "mixed-metal phase" to be identified from either binary (Figure S3) or ternary oxalates (Figure S4). The quantitative evaluation of the spectra, along with the associated H_2 consumption (Figure S3), demonstrated the CoCu mixed phase to be metallic. However,

in the ternary decomposition product, oxygen was retained after H_2-TPDec (Figure S4). Thus, Mn-oxalate did not reduce to a metallic state, which is in agreement with what the literature reports.[11] On the other hand, the oxygen remainders did not prevent the activated catalysts from being pyrophoric and caused a drastic increase in the specific surface area from 10 m^2/g in Co_1Cu_1 to 170 m^2/g in $Co_1Cu_1Mn_1$. Thus, catalysts had to be passivated before characterization or transfer into the reactor.

One of the attractive features of the oxalate route of catalyst preparation is that no classical support material is needed. There are indications from transmission electron microcopy (TEM) that some phase separation occurs during the thermal decomposition of the ternary oxalate precursor. Besides "CoCuMn" which is largely metallic as shown below, a distinct (catalytically inactive) Mn-oxide phase is likewise identified (see SI). It should also be noted that according to the phase diagram of binary Co−Cu only a maximum of 9 at% Cu can be dissolved in Co metal.[12] According to the ternary Co−Cu−Mn phase diagram, the large Co−Cu miscibility gap can be reduced through the addition of Mn.[13] These thermodynamic considerations are in line with the hypothesis that an intimate mixing of the metals is key to boosting the selective formation of long-chain hydrocarbons with terminal functionalization.[9]

As mentioned above, the notion "CoCuMn" suggests the occurrence of a largely metallic phase with all three metals being present in the same particles. To demonstrate this, we present in Figure 1 for the first time atom maps recorded from
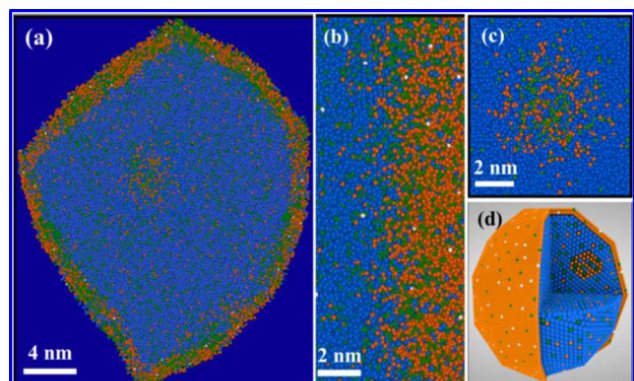

Figure 1. (a) Atom probe microscopy results from the CoCuMn catalyst nanoparticles. The images provided here are sections through 3D tomographic reconstructions so as to reveal the intragranular structure of the nanoparticles. The data are presented in the form of atom maps where Co atoms are depicted as blue spheres, Cu atoms as orange spheres, Mn atoms as green spheres, and O as white spheres. A faceted core−shell structure that contained intracore clusters was observed. The data displayed are from a 10 nm thick slice through one grain. (b) An enlarged view from a 5 nm thick slice of the data at the core−shell interface. Oxygen (white) was distributed throughout the core−shell interface. (c) The intracore clusters were observed to contain a high concentration of Cu and Mn; 5 nm thick atom map. (d) A 3D sectional view of the element distribution.

a single CoCuMn catalyst grain using atom probe tomography (APT). For these experiments a passivated sample of the catalyst was conditioned to form a nanosized tip (see SI) which was subjected to laser-assisted field evaporation. To recall, APT consists in the atom-by-atom removal of the sample as ions. After their arrival at a position-sensitive detector the original sample is 3D-reconstructed. The results provide a striking

demonstration of the core−shell chemical structure, with major amounts of Co forming the core, and all three elements are clearly present in an otherwise Cu-dominated outer shell of about 2 nm thickness. Our synthesis also stimulates the formation of very small nanosized CoCuMn precipitates, which occur inside the core structure (Figure 1c). Furthermore, only small amounts of oxygen are detected. We therefore conclude that the CoCuMn phase is largely metallic and it may be suspected, without consideration of a possible reaction-induced reconstruction, that with such phase composition electronic ligand effects will become important during FT synthesis.

We now turn to the catalytic performance of "CoCuMn" and start by comparing it with that of "CoCu". In Figure 2, this
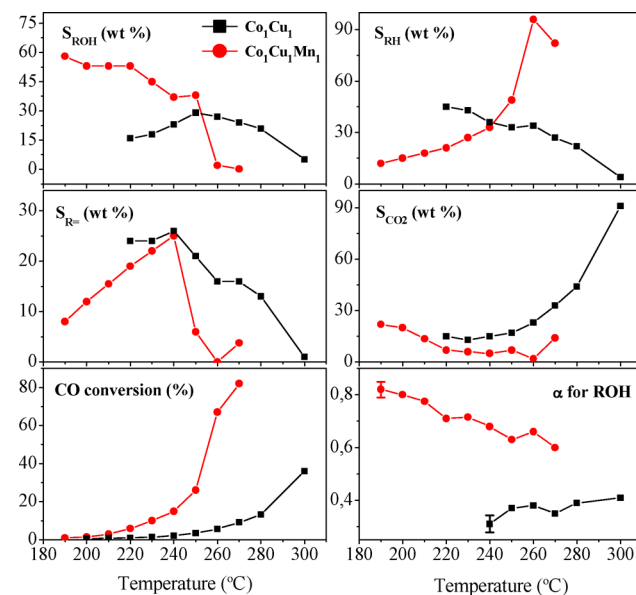

Figure 2. Catalytic performance of Co_1Cu_1 and $Co_1Cu_1Mn_1$ catalysts during the FT reaction. Catalytic tests were carried out at $p = 60$ bar and $H_2/CO = 2$ for 24 h each. Errors for chain lengthening are calculated from the deviations of $\log(W_n/n)$ versus n from linearity. $W_n = n(1 − \alpha)^2\alpha^{n-1}$, where W_n stands for the mass fraction of products containing n carbon atoms. Higher conversion increases the statistical significance and, accordingly, reduces the error.

comparison is made in terms of activity, selectivity and α-ASF chain-lengthening probability for Co_1Cu_1 and $Co_1Cu_1Mn_1$. It is obvious that both catalysts are active in terminal alcohol and olefin production. While the ROH selectivity (S_{ROH}) increases with decreasing reaction temperatures for $Co_1Cu_1Mn_1$, it runs through a broad maximum at around 250 °C for Co_1Cu_1. S_{ROH} values of close to 60% at otherwise low CO conversion are obtained for $Co_1Cu_1Mn_1$ at 190 °C, while for Co_1Cu_1 the maximum S_{ROH} is considerably lower and reaches about 30% at the most. It is also obvious from Figure 2 that the enhanced 1-alcohol selectivity entails a respective decrease in the n-alkane (S_{RH}) and 1-alkene ($S_{R=}$) selectivity for $Co_1Cu_1Mn_1$. This trade-off between S_{ROH} and ($S_{RH} + S_{R=}$) is not observed for Co_1Cu_1. The selectivity performance of the binary catalyst is therefore much less pronounced than that of ternary $Co_1Cu_1Mn_1$.

CO_2 production is unwanted but frequently reported to be difficult to control.[14] In the present case, the selectivity in terms of CO_2 (S_{CO_2}) is quite low for $Co_1Cu_1Mn_1$ over a range of temperatures. Under conditions of increasing CO conversion,

an enhanced CO_2 production is frequently related to the occurrence of the water-gas shift reaction, $CO + H_2O \rightarrow CO_2 + H_2$, which may be beneficial if feeds with higher than nominal H_2/CO ratios are required. In the present case, for $Co_1Cu_1Mn_1$, the strong increase in the CO conversion above 250 °C does not entail drastic changes in the CO_2 production. Changing selectivity patterns in favor of hydrocarbon production at high temperatures must therefore be attributed to intrinsic kinetic effects of the FT reaction, rather than to the water–gas shift reaction. It is also clear from Figure 2 that Co_1Cu_1 produces mainly CO_2 in the upper temperature range, without concomitant hydrocarbon formation.

The most intriguing observation in Figure 2 is the high α-ASF chain-lengthening probability for 1-alcohol formation of the $Co_1Cu_1Mn_1$ catalyst. The α-values range from 0.6 to above 0.8 for temperatures between 270 and 190 °C and therefore achieve the purpose of maximizing the yields of C_8-C_{14} terminal alcohols. The corresponding ASF chain-lengthening distributions are linear for both $Co_1Cu_1Mn_1$ and Co_1Cu_1 (Figure S5); however, the latter catalyst fails to produce the envisaged C_8-C_{14} slate of terminal alcohols. Instead, Co_1Cu_1 shows a chain-lengthening probability of 0.31 suitable for short-chain alcohol production up to about C_6, which is what the literature reports for either supported or unsupported CoCu catalysts.[14−16]

The $Co_1Cu_1Mn_1$ case study is encouraging with respect to a possible industrial application. From this point of view it is fair to consider the sum yield of terminal alcohol and olefin production. According to Figure 2, $Co_1Cu_1Mn_1$ provides a combined ROH/R= selectivity of about 60% at a CO conversion level of 18%, while the loss in terms of CO_2 is below 10% at 240 °C. Furthermore, a unique α-value of 0.69 at this temperature seems ideal to meet the requirement for an optimum 1-alcohol slate in the range C_8-C_{14}. Therefore, we decided to perform detailed studies of the catalytic performance of this ternary system by changing the relative amounts of Mn in "CoCuMn" from 1 to 0.1 for both Co_1Cu_1 and Co_1Cu_4. The results are shown in Figure 3. Generally, high CO conversion can only be reached at sufficiently high temperatures, with major changes occurring in the range between 240 and 260 °C, depending on the catalyst composition. The selectivity patterns of the various catalysts change accordingly; all catalysts were selective in 1-alcohol/1-alkene production at low temperatures while they were more selective in n-alkane production at higher temperatures. Large amounts of unwanted CO_2 were only observed for $Co_1Cu_4Mn_1$ catalysts above 240 °C.

The highest S_{ROH} value was observed for $Co_1Cu_4Mn_{0.1}$ under conditions of low CO conversion. Actually, the sum of S_{ROH} and $S_{R=}$ for this catalyst was above 95%, with negligible CO_2 formation. This selectivity pattern is close to ideal; however, the catalyst activity is insufficient. A good compromise between activity and ROH/R= selectivities is presently only obtainable at medium temperatures around 240 °C. The $Co_1Cu_1Mn_1$ catalyst still performs best at this point in time and appears to be a suitable candidate for further optimization.

Another interesting feature emerges by inspecting the α-ASF chain-lengthening probabilities in Figure 3. Despite the trade-off between ROH/R= and RH selectivities, the general trend appears to be that the α-values increase for all products with decreasing temperatures. Except for some fluctuations associated with $Co_1Cu_4Mn_1$, all catalysts behave similarly in this respect. The same holds while varying the overall pressure conditions, partial pressure ratios, and contact times (for
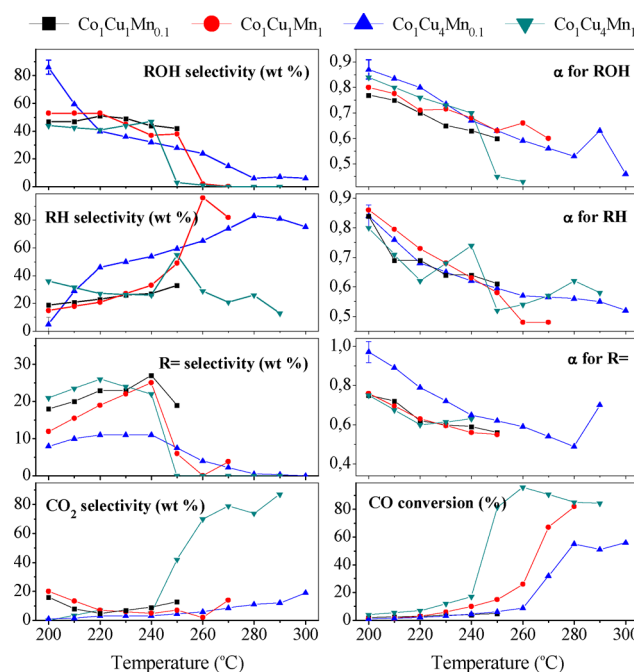

Figure 3. FT activity and selectivity performance for "CoCuMn" catalysts with varying relative amounts of metal atoms. The same pressure and time-on-stream conditions apply as in Figure 2. We also note that only the $Co_1Cu_1Mn_x$ catalysts are diluted with SiC while $Co_1Cu_4Mn_x$ are not, due to the high heat conductivity of these samples. Error bars for selectivities (at low conversion) indicate the spread of data in three independent measurements with three catalysts of identical composition. Data points are the arithmetic means calculated from these measurements. Error bars for α-values are calculated as in Figure S5.

performance data see Figure S6) for $Co_1Cu_1Mn_1$. The observation of correlated α-values for varying catalyst compositions and reaction conditions would be in accordance with a common chain-growth mechanism through CO-insertion into the same type of precursor intermediateand a late kinetic branching to n-alkanes, 1-alcohols, and 1-alkenes. However, the currently most accepted view is hydrocarbon chain lengthening to proceed via polymerization of CH_x building blocks or, more specifically, via CH_2 monomer insertion into surface-alkyl and oxygenate production to involve CO insertion at different catalytic sites.[17] While the present work was not intended to cast additional light on this matter, it should be mentioned that recent transient kinetic research on the atmospheric CO hydrogenation over various model catalysts including CoCu brought forth,[18] in accordance with the observation of a hydrogen-assisted CO dissociation in the early stages of the reaction,[19] that hydrocarbons are formed in a chain lengthening mechanism involving CO insertion.[20] It is interesting to note in this context that the homogeneous hydroformylation is essentially accepted to proceed via CO insertion into a metal−alkyl bond (alkyl shift) since the early mechanistic work of Heck and Breslow.[8]

To summarize, we have demonstrated here that FT catalysts can be designed to produce long-chain terminal alcohols with high selectivity from syngas. Using "CoCuMn" catalysts with core−shell structure, we have been able to adjust the α-ASF chain lengthening probability to optimize the yield of the C_8-C_{14} product slate as feedstock for plasticizers, lubricants, detergents etc. in a "one-step, one-pot" process. There is no

doubt that the unconventional, though "relatively simple", oxalate route of catalyst preparation plays an important role in designing mixed-metal catalysts free of a classic support while ensuring high specific surface areas through a dispersion effect and providing promotional interaction of the Mn with the CoCu mixed surface phase. Most of the present-day research on C_{2+}-mixed alcohol formation (see also Table S1) is focused on optimizing the C_2–C_6 rather than the C_{7+} slate by using more conventional metal-oxide supported CoCu catalysts.[15] The structural and textural properties of these catalysts are quite different from "CoCuMn" as developed in our work, making a comparison somewhat difficult. Our design strategy has allowed the creation of nanoscale catalyst particles that possess a Co-rich core structure and a Cu-dominated CoCuMn mixed shell that is highly effective in enabling chain lengthening with terminal alcohol or olefin production. More recent work on bimetallic CoCu[16] has reported on the catalytic performance of supposedly Co@Cu core–shell as well as CoCu mixed nanoparticle structures in the absence of a support. Both types of catalyst seem to produce various oxygenates (aldehydes, ketones, alcohols) up to C_4 along with large amounts of CO_2. The performance of CoCu nanoparticles (1:24 at%) in terms of activity and selectivity to alcohols comes close to that obtained for CoCu (1:1 at%) mixed-phase particles, as used in our work. As we have seen, "CoCuMn" demonstrates a performance, though not yet ideal, that is clearly superior to CoCu at a benchtop level, and so appears to have considerable potential for application to the large-scale industrial production of long-chain terminal alcohols via the heterogeneous CO hydrogenation—as first contemplated by Roelen, about 75 years ago.

■ ASSOCIATED CONTENT

Ⓢ Supporting Information

Experimental procedures, Figures S1–S6, and Table S1. This material is available free of charge via the Internet at http://pubs.acs.org.

■ AUTHOR INFORMATION

Corresponding Author

nkruse@ulb.ac.be

Notes

The authors declare no competing financial interest.

■ ACKNOWLEDGMENTS

■ REFERENCES

(1) Eilbracht, P.; Bärfacker, L.; Buss, C.; Hollmann, C.; Kitsos-Rzychon, B. E.; Kranemann, C. L.; Rische, T.; Roggenbuck, R.; Schmidt, A. *Chem. Rev.* **1999**, *99*, 3329.

(2) Dong, G.; Teo, P.; Wickens, Z. K.; Grubbs, R. H. *Science* **2011**, *333*, 1609.

(3) (a) Cole-Hamilton, D. J. *Science* **2003**, *299*, 1702. (b) Boogaerts, I. I. F.; White, D. F. S.; Cole-Hamilton, D. J. *Chem. Commun.* **2010**, *46*, 2194. (c) Fuchs, D.; Rousseau, G.; Diab, L.; Gellrich, U.; Breit, B. *Angew. Chem., Int. Ed.* **2012**, *51*, 2178.

(4) (a) Takahashi, K.; Yamashita, M.; Ichihara, T.; Nakano, K.; Nozaki, K. *Angew. Chem., Int. Ed.* **2010**, *49*, 4488. (b) Takahashi, K.; Yamashita, M.; Nozaki, K. *J. Am. Chem. Soc.* **2012**, *134*, 18746.

(5) Fischer, F.; Tropsch, H. *Brennst. Chem.* **1923**, *4*, 276.

(6) Roelen, O., German Patent 849 548, 1938.

(7) Wender, I.; Sternberg, H. W.; Orchin, M. *J. Am. Chem. Soc.* **1953**, *75*, 3041.

(8) Heck, R. F.; Breslow, D. S. *J. Am. Chem. Soc.* **1961**, *83*, 4023.

(9) (a) Buess, P.; Caers, R. F. I.; Frennet, A.; Ghenne, E.; Hubert, C., Kruse, N. U.S. Patent 6 362 239 B l, 2002. (b) Frennet, A.; Hubert, C.; Ghenne, E.; Chitry, V.; Kruse, N. *Stud. Surf. Sci. Catal.* **2000**, *130*, 3699.

(10) García-Couceiro, U.; Castillo, O.; Luque, A.; Beobide, G.; Román, P. *Inorg. Chim. Acta* **2004**, *357*, 339.

(11) Iablokov, V.; Frey, K.; Geszti, O.; Kruse, N. *Catal. Lett.* **2010**, *134*, 210.

(12) Predel, B. In *Co-Cu (Cobalt-Copper)*; Madelung, O., Ed.; SpringerMaterials—The Landolt-Börnstein Database, Vol. 5C: Ca-Cd — Co-Zr; http://www.springermaterials.com, 2013, DOI: 10.1007/10086082_908.

(13) Materials Science International Team; Bochvar, N.; Lysova, E.; Rokhlin, L. In *Co-Cu-Mn (Cobalt-Copper-Manganese)*; Effenberg, G., Ilyenko, S., Eds.; SpringerMaterials—The Landolt-Börnstein Database, Vol. 11C3: Non-Ferrous Metal Systems; http://www.springermaterials.com, 2013, DOI: 10.1007/978-3-540-47004-5_23, p 212.

(14) (a) Sugier, A.; Freund, E. U.S. Patent 4 122 110, 1978. (b) Courty, P.; Durand, D.; Freund, E.; Sugier, A. *J. Mol. Catal.* **1982**, *17*, 241.

(15) (a) Wang, J.; Chernavskii, P. A.; Khodakov, A. Y.; Wang, Y. *J. Catal.* **2012**, *286*, 51. (b) Bailliard-Letournel, R. M.; Gomez Cobo, A. J.; Mirodatos, C.; Primet, M.; Dalmon, J. A. *Catal. Lett.* **1989**, *2*, 149. (c) Mo, X.; Tsai, Y.-T.; Gao, J.; Mao, D.; Goodwin, J. G., Jr *J. Catal.* **2012**, *285*, 208.

(16) Subramanian, N. D.; Balaji, G.; Kumar, C. S. S. R.; Spivey, J. J. *Catal. Today* **2009**, *147*, 100.

(17) (a) Fischer, F.; Tropsch, H. *Brennst. Chem.* **1926**, *7*, 97. (b) Chuang, S. C.; Tian, Y. H.; Goodwin, J. G., Jr; Wender, I. *J. Catal.* **1985**, *96*, 396. (c) Ponec, V. *Catal. Today* **1992**, *12*, 227. (d) Dry, M. E. *Appl. Catal. A: Gen.* **1996**, *138*, 319. (e) Schulz, H. *Top. Catal.* **2003**, *26*, 73. (f) van Dijk, H. A. J.; Hoebink, J. H. B. J.; Schouten, J. C. *Top. Catal.* **2003**, *26*, 111. (g) Davis, B. H. *Catal. Today* **2009**, *141*, 25. (h) Cheng, J.; Hu, P.; Ellis, P.; French, S.; Kelly, G.; Lok, C. M. *Top. Catal.* **2010**, *53*, 326. (i) Visconti, C.; Tronconi, E.; Lietti, L.; Forzatti, P.; Rossini, S.; Zennaro, R. *Top. Catal.* **2011**, *54*, 786. (j) van Santen, R. A.; Ciobîcă, I. M.; van Steen, E.; Ghouri, M. M. *Adv. Catal.* **2011**, *54*, 127.

(18) (a) Frennet, A.; Visart de Bocarmé, T.; Bastin, J.-M.; Kruse, N. *J. Phys. Chem. B* **2004**, *109*, 2350. (b) Bundhoo, A.; Schweicher, J.; Frennet, A.; Kruse, N. *J. Phys. Chem. C* **2009**, *113*, 10731.

(19) (a) Ojeda, M.; Nabar, R.; Nilekar, A. U.; Ishikawa, A.; Mavrikakis, M.; Iglesia, E. *J. Catal.* **2010**, *272*, 287. (b) Tuxen, A.; Carenco, S.; Chintapalli, M.; Chuang, C.-H.; Escudero, C.; Pach, E.; Jiang, P.; Borondics, F.; Beberwyck, B.; Alivisatos, A. P.; Thornton, G.; Pong, W.-F.; Guo, J.; Perez, R.; Besenbacher, F.; Salmeron, M. *J. Am. Chem. Soc.* **2013**, *135*, 2273.

(20) Schweicher, J.; Bundhoo, A.; Kruse, N. *J. Am. Chem. Soc.* **2012**, *134*, 16135.